PROPAGATION OF FLARE PROTONS IN THE SOLAR ATMOSPHERE

R. REINHARD and G. WIBBERENZ
Institut für Reine und Angewandte Kernphysik, Universität Kiel, W. Germany

(Received 20 August, 1973; in revised form 19 February, 1974)

Abstract. The velocity dispersion for a large number of solar proton events is analyzed in the energy regime of 10–60 MeV. It is found for all events that the time from the flare to particle maximum t_m is well represented by a sum of two components. The first component which is energy independent describes the propagation in the solar atmosphere, the second component describes the propagation in the interplanetary medium giving a velocity dispersion $v \times t_m = \text{const}$. The additional study of time intensity profiles, onset times, and multispaceprobe observations reveals that the propagation in the solar atmosphere consists of three processes: (1) A rapid transport process in the initial ($\lesssim 1$ h) phase after the event fills up a "fast propagation region (FPR)", which may extend up to $\approx 60°$ from the flare site and which is tentatively identified with a large unipolar magnetic cell as seen on Hα synoptic charts, (2) a large-scale drift process which is energy independent with drift velocities v_D in the range $1° \leqslant v_D \leqslant 4°$ h^{-1}, and simultaneously (3) a diffusion process which yields the general broadening of the intensity time profiles for eastern hemisphere events, which is, however, of less importance than previously assumed.

1. Introduction

The propagation of energetic solar flare accelerated particles from the flare location to the Earth is a result of solar and interplanetary propagation processes which are difficult to separate. There appears to be good evidence, however, to suggest a diffusion region around the Sun (Reid, 1964; Axford, 1965; Fan *et al.*, 1968; Simnett, 1971). One of the more important results which support this concept is the broad longitudinal range over which solar particles are observed at the orbit of Earth for a given flare (Bukata *et al.*, 1972) and the apparently low rate of longitudinal diffusion of solar cosmic rays across the spiral interplanetary magnetic field lines. The predominantly one-dimensional character of the diffusion along these field lines is strongly supported by the large field aligned anisotropies during the early phase of an event. The first particles usually arrive from a westerly direction independent of the solar flare longitude (Rao *et al.*, 1971 and ref. therein).

Further confirmation was obtained by the observed clear differences in the particle ($E_p \geqslant 0.3$ MeV) onset times at different spacecraft, even when they are relatively close to the same magnetic field line (Krimigis *et al.*, 1971). The fact that identifiable features in the particle intensity profile can often be observed by widely separated spacecraft (>0.1 AU) with a delay time expected from corotation (Krimigis *et al.*, 1971) would be difficult to understand if transverse diffusion would play an important role.

The interplanetary magnetic field lines are twisted and have numerous irregularities which scatter the particles. Solar flare accelerated particles span a wide range of Larmor radii. Accordingly, magnetic field fluctuations over a wide range of scale

Solar Physics **36** (1974) 473–494.

sizes will be responsible for particle scattering. Under this circumstance it is remarkable that for a number of events the propagation has been found to be velocity dependent only. In a technique first employed by Bryant *et al.* (1965) the intensity distance profile was analyzed by plotting the intensity as a function of $v \times t$, which is the distance travelled by a particle group with velocity v after a time t measured from the time of acceleration at the Sun. It was found that the intensity as a function of distance had nearly the same profile for proton energies from a few up to several hundred MeV.

Cline and McDonald (1968) showed that for the July 7, 1966 event this behaviour could be extended to relativistic electrons. If interpreted in terms of a diffusion model with a constant mean free path between source and observer, this event would be represented by $\lambda = 0.05$ AU. The authors point out, however, that the observed velocity dispersion only indicates that the various particle groups have travelled the same distance, and that the result does not give information about *where* most of the propagation occurred.

The technique of plotting the normalized intensity vs $v \times t$ has meanwhile been used by many authors (e.g. Barcus, 1969; Barouch *et al.*, 1969; Lin, 1970; Dilworth *et al.*, 1972). It was found that some events can be described by pure velocity dispersion and others not.

It is one of the purposes of this paper to study the velocity dependence of a large number of events in more detail. It will be shown that in general there is a remarkable difference in the velocity dispersion of western and eastern hemisphere events. These differences have a simple explanation in terms of different propagation processes in the solar atmosphere and in the interplanetary medium.

2. Data Analysis

The particle data on which the results are mainly based were taken from the Solar Proton Monitor Experiment (SPME) on IMP F and G by Bostrom *et al.* during the period May 1967 through May 1972. The hourly averages of the >10, >30 and >60 MeV protons are published monthly in the *Solar Geophysical Data* (cf. ref.). During this time 132 well-defined intensity increases in the >10 MeV proton channel were observed. Further analysis was restricted to events, where:

(1) we could make a *very reliable* flare association,

(2) the rise time is shorter than the decay time,

(3) the fluctuations in the time intensity profile are not too strong,

(4) the spectral exponent of $\mathrm{d}j/\mathrm{d}E \sim E^{-\gamma}$ clearly satisfies $\gamma \lesssim 5$ at the time of maximum particle intensity.

The number of events was further reduced by satellite magnetospheric passages.

Condition 3 is necessary since we are mainly concerned in this paper with particle onset and maximum intensity times, which must be clearly identifiable. Conditions 1, 2, and 4 should exclude corotating or other not flare induced events.

The time difference between the acceleration of energetic particles at the flare site

and the maximum particle intensity at the satellite is called t_m. The time of particle acceleration is taken as the maximum of the Hα-flare intensity minus 10 min, taking into consideration the travel time of light of 8.3 min for 1 AU and the fact that the flash phase occurs a few minutes before the Hα-maximum.

Many observations have established that t_m increases with the azimuthal distance from the flare $\Delta\phi$ (east-west effect). This effect is explained by anisotropic propagation of cosmic ray particles with respect to the average magnetic field direction. There is a large variety of theoretical models which describe the east-west effect properly, even under markedly different model assumptions, such as the relative importance of azimuthal particle transport close to the Sun and particle transport perpendicular to the interplanetary magnetic field. This is possible by a suitable fit of the model parameters. The remaining differences between the models are smaller than the scatter of observed t_m values at a given longitude. The east-west effect, therefore, is not a significant test for the different model assumptions.

It is also predicted by theoretical models that t_m has a minimum at a particular solar longitude. The ADB model proposed by Burlaga (1967) has the minimum around W 60°, with a small scatter due to the variations of the solar wind velocity. According to Englade's calculation (1971) the minimum should be around W 22°. The eastward shift in comparison to Burlaga's model is connected with the inclusion of the spiral shape of the interplanetary field lines.

Plotting observed t_m data Datlowe (1971) concludes that there is a minimum at W 35° for 90–110 MeV protons and at W 30° for 15–45 MeV electrons. Barouch *et al.* (1971) studied the onset times of 6–25 MeV protons and obtained a minimum value at W 45°. When Simnett (1971) studied the onset times of 0.3–0.9 MeV electrons, he found the smallest times in a region W 30°–W 60°. McKibben (1972) analyzed the times of maximum particle intensity for 15–18.7 MeV protons simultaneously with Pioneer 6 and 7 and IMP F. His plot of $t_m(\phi)$ indicates that the sector for small t_m values ranges from W 10°–W 100°. Sakurai (1971) finds the smallest times at W 30° and at W 80° in his study of transit times (t_s) of >20 keV electrons. A somewhat more extended analysis carried out by Obayashi (1964) shows minimum values of t_s for PCA events extending from W 10° to W 90°. To summarize, there is no clear indication for a pronounced minimum in the propagation times at a particular solar longitude. Especially, if all these observations are combined, we find that small t_m values are equally likely to occur over a wide range of solar longitude on the western hemisphere of the Sun.

Figure 1 shows $t_m(\phi)$ for the >10, >30 and >60 MeV protons. The data points are bounded by lines, that indicate the region of ≈0°–W 100°, where minimum t_m values are observed. It is obviously impossible to determine a particular solar longitude for the smallest time to maximum; on the contrary, the smallest values are observed at W 30° and at W 90°, at longitudes, which are 60° apart.

The lateral extent of the region is independent of the particle energy at least in the energy regime, which is under discussion here. There is significant scatter in the t_m values at a given solar longitude which at least partly reflects the different inter-

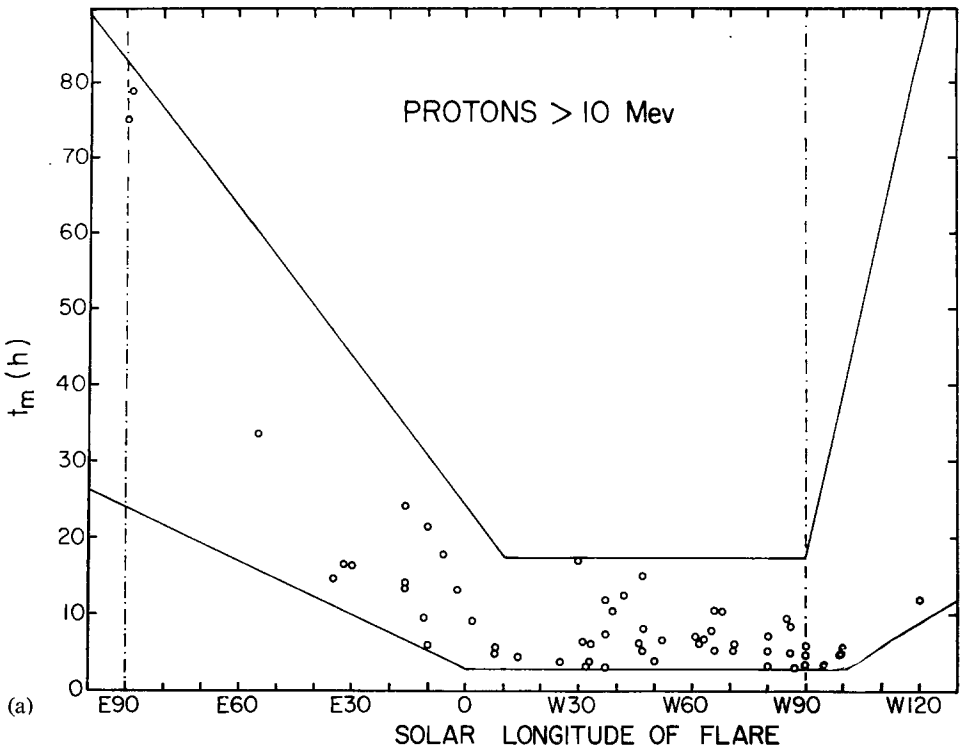
PROTONS > 10 Mev
t_m (h)
0
10
20
30
40
50
60
70
80
E90
E60
E30
0
W30
W60
W90
W120
SOLAR LONGITUDE OF FLARE

(a)

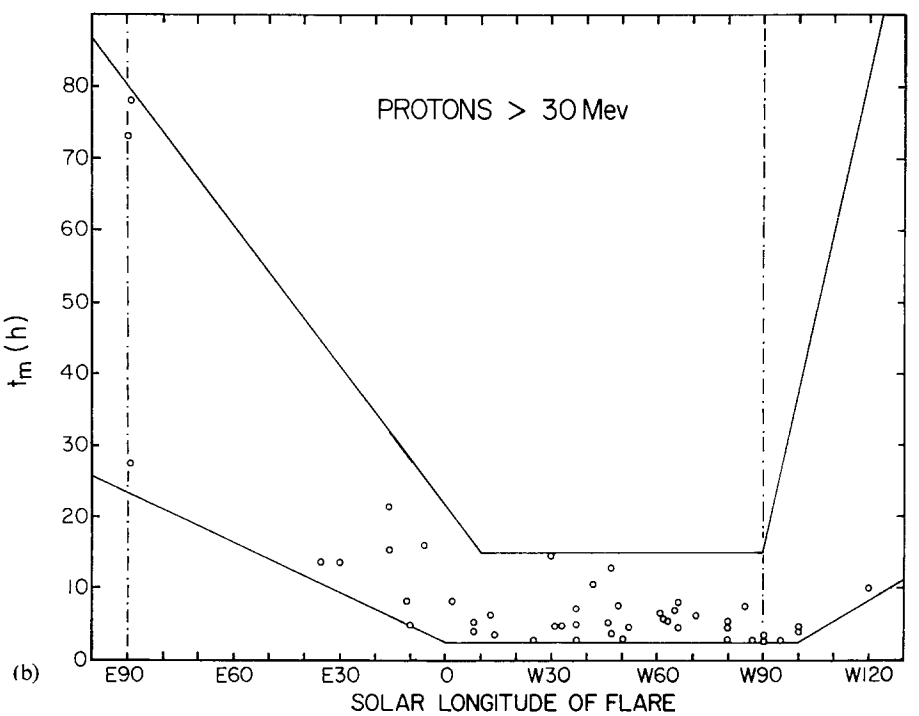
PROTONS > 30 Mev
t_m (h)
0
10
20
30
40
50
60
70
80
E90
E60
E30
0
W30
W60
W90
W120
SOLAR LONGITUDE OF FLARE

(b)

Figs. 1a, b.

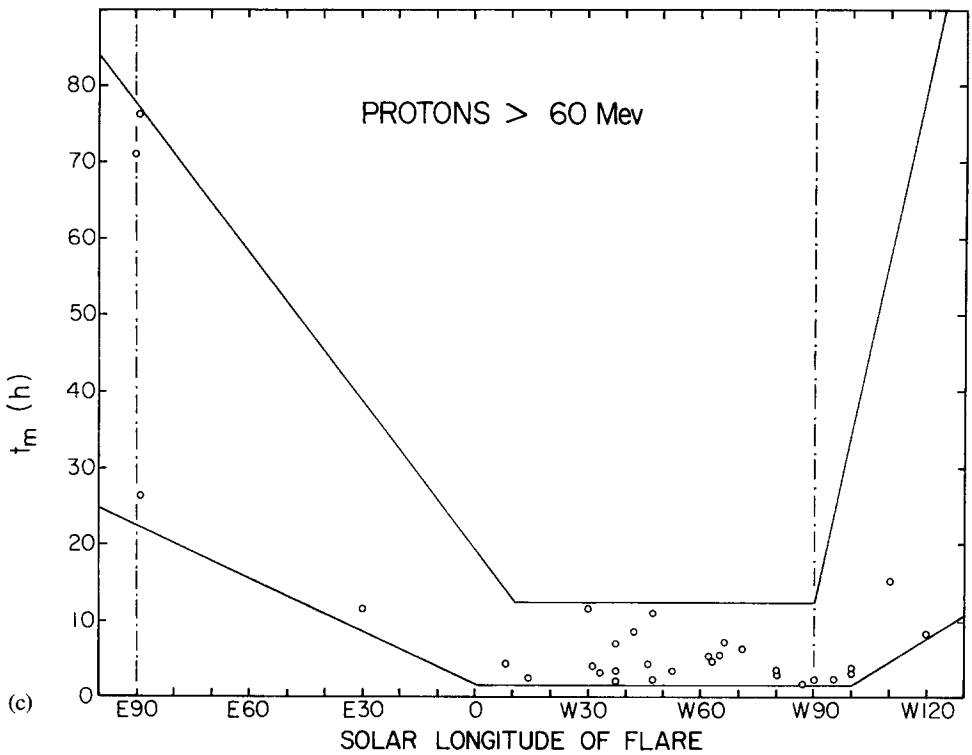

Figs. 1a–c. The time difference between the maximum particle intensity at the spacecraft and the time of acceleration at the flare site vs the solar longitude of the flare for (a) > 10, (b) > 30, and (c) > 60 MeV protons. The time of acceleration is assumed to be the observed time of the Hα maximum minus 10 min. Note that there is no t_m minimum at a particular solar longitude.

planetary propagation conditions from one event to the other. The lateral extent of the sector is chosen differently for the upper and lower line to indicate the variability of the extent.

It can be seen from Figure 1 that the t_m values are generally smaller for the higher particle energies giving evidence for the velocity dispersion effect. All events fall well within bordering lines with slopes in the eastern hemisphere that are identical for the 3 energy ranges. The fact that the slopes are independent of energy indicates that the difference in the t_m values between the various energies is independent of longitude. This observation will be discussed below in more detail. The corotation effect would correspond to a westward shift in longitude of 13.3° day^{-1}; this means that events from the invisible disk are less favourably located to be observed at Earth than easterly events equally distant from W 60°. Correspondingly, the slopes of the bordering lines for the events beyond W 90° are steeper taking the corotation effect into account.

3. Velocity Dependence and Interplanetary Propagation

To further analyze the observed longitudinal dependence we compare the time intensity profiles of different energies for a given flare event in detail (October 4, 1968, W 37°; Figure 2). The time of maximum intensity increases systematically with decreasing energy, according to $v \times t_m = 8.3$ AU. v is the particle velocity of the 10, 30, and 60 MeV protons respectively, assuming a sufficiently steep energy spectrum,

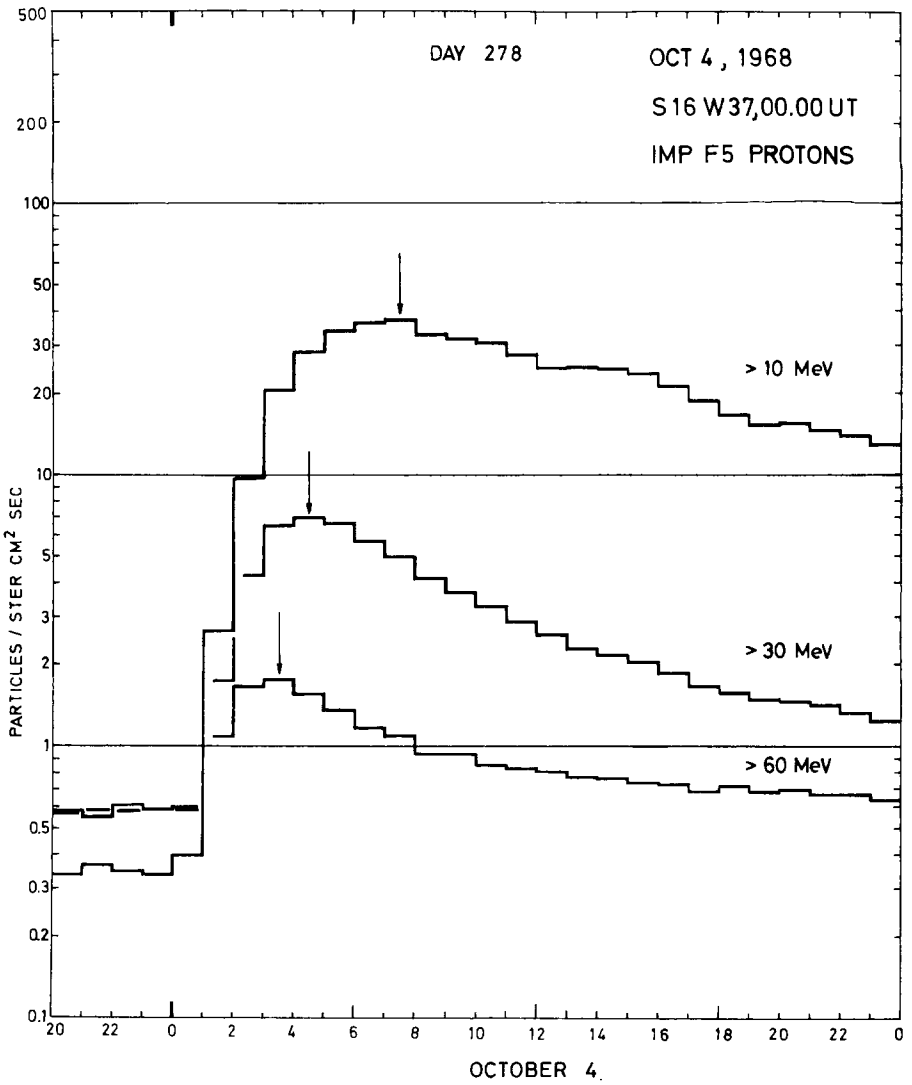

Fig. 2. The October 4, 1968, W 37° event is shown as an example for a typical velocity dispersion event, i.e. $v \times t_m = \text{const}$. IMP F 5 describes the spacecraft and the experiment F 5 according to the NSSDC nomenclature. Also given is the acceleration time of 00 UT.

so that the counting rate is mainly determined by particles close to the lower threshold energy.

The flare, which produced the velocity dependent time intensity profiles in Figure 2, is located at W 37°. There is a large number of events in the western hemisphere with $v \times t_m = \text{const}$. The mean travelled distances range from ≈ 2 AU (March 24, 1966, W 42°) to ≈ 10 AU (e.g. July 7, 1966, W 48°).

Events in the eastern hemisphere in general show a typically different behaviour, especially if they are located close to the east limb of the Sun. As an example we plotted the time intensity profiles of the December 2, 1968 event which occurred at E 89° (Figure 3). This event was chosen because of its relatively undisturbed profile near maximum. The kink in the rise does not influence our interpretation since the time differences between the maxima are roughly the same as for other east limb events. We find in this case (see insert, Figure 3)

$$\begin{aligned} &10 \text{ MeV}: \quad t_m = 78 \text{ h}, \quad v_{10} \times t_m = 82 \text{ AU}, \\ &30 \text{ MeV}: \quad t_m = 76 \text{ h}, \quad v_{30} \times t_m = 136 \text{ AU}, \\ &60 \text{ MeV}: \quad t_m = 75 \text{ h}, \quad v_{60} \times t_m = 185 \text{ AU}, \end{aligned}$$

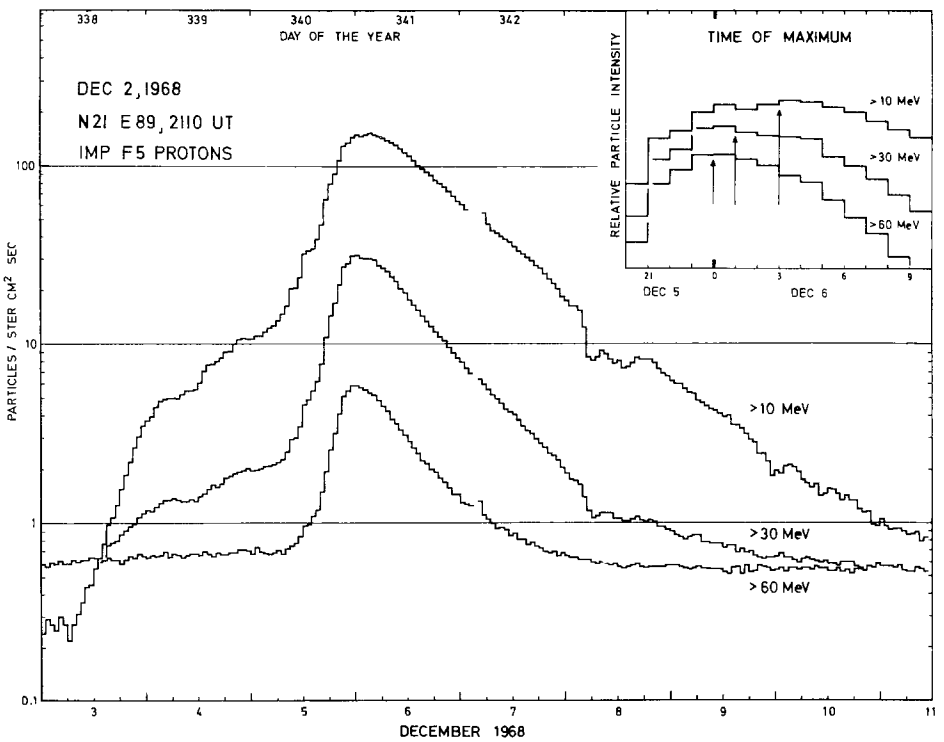

Fig. 3. The December 2, 1968, E 89° event is shown as an example for an east-limb event. The insert shows the normalized particle intensity for the time around particle intensity maximum. The time differences between the maxima for the 3 energies are roughly the same as for the event in Figure 2

which clearly is a systematic increase of $v \times t_m$ with the particle energy. The *absolute* time differences between the particle intensity maxima, however, are of the same magnitude as for the western hemisphere event in Figure 2. Analyzing a large number of events this result can be generalized: on the average, the time differences between the particle intensity maxima belonging to different energies are independent of the solar longitude, whereas the absolute value of t_m increases with the solar longitude,

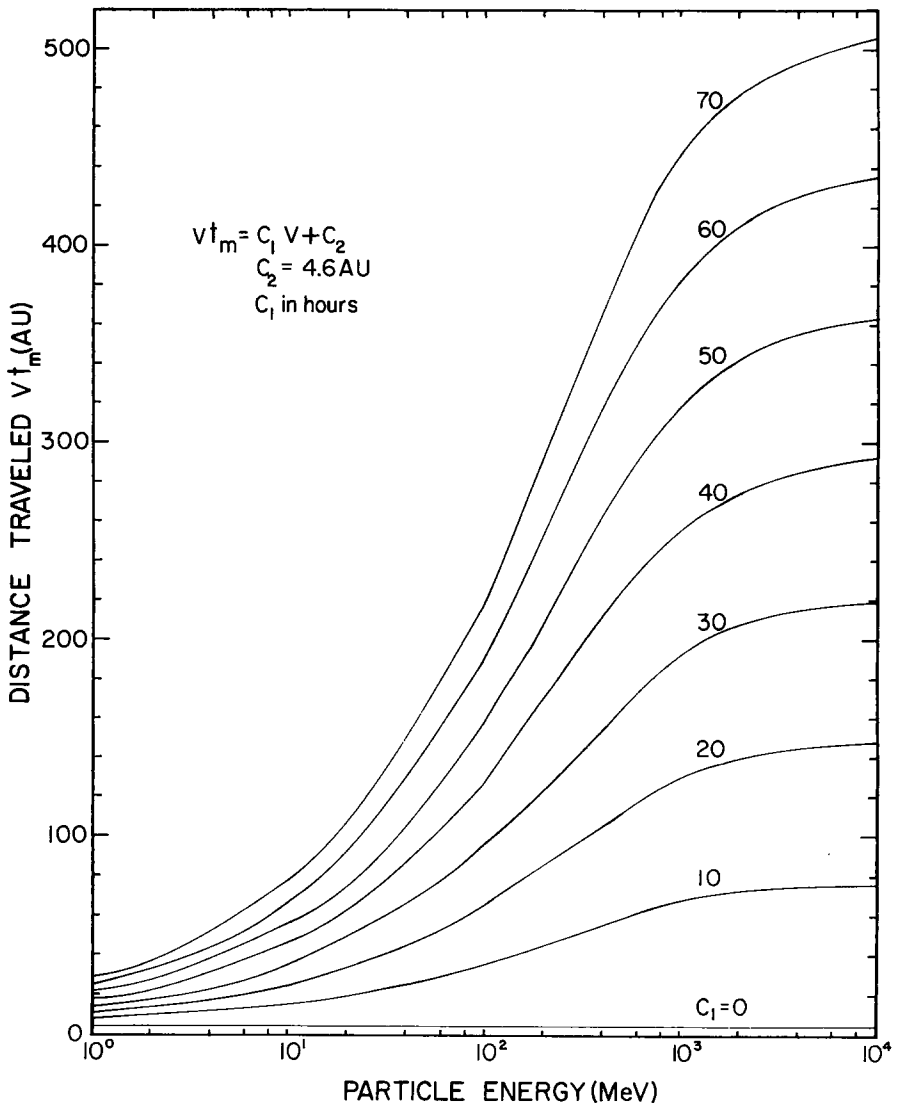

Fig. 4. The travelled distance $v \times t_m$ vs particle energy assuming that the variation of t_m is described by $t_m = c_1 + c_2/v$ with c_1 as parameter. An average value of $c_2 = 4.6$ AU (see Figure 8) has been taken for all the curves. The flattening for energies $\gtrsim 10^3$ MeV is due to $v \to c$, the velocity of light.

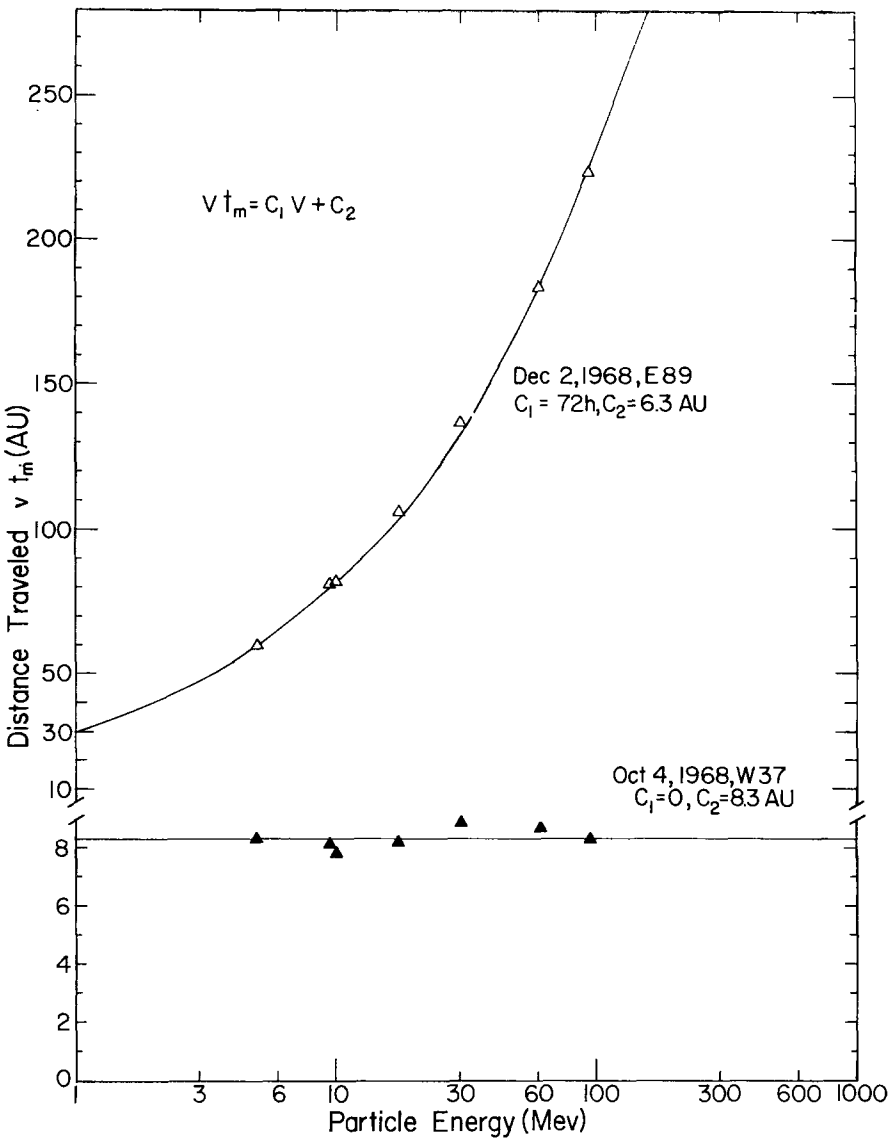

Fig. 5. Fit of the 2 events from Figures 2 and 3 to Equation (1) with parameter values c_1 and c_2 as indicated.

independent of the particle energy. It is found that the variation of t_m with velocity and flare location for *all* events can be described by

$$t_m = c_1(\phi) + c_2/v, \tag{1}$$

where c_1 and c_2 are characteristic constants for one event. The second component is responsible for the observed velocity dispersion. If $c_1 = 0$, we have pure velocity

dispersion, as for example the October 4, 1968 event ($c_2 = 8.3$ AU). c_1 is the energy independent part of t_m, which increases with solar longitude $\Delta\phi$, where $\Delta\phi$ is measured relative to the footpoint of the spiral magnetic field line connecting the Earth with the Sun. For large $\Delta\phi$, that is for eastern hemisphere events, the first component is the dominating part of t_m.

If we plot the $v \times t_m$ values obtained for one event vs the particle energy E we get a straight line parallel to the E-axis for all events with pure velocity dispersion. Figure 4 shows the curves representing the above equation with c_1 as parameter. c_2 is taken as 4.6 AU, the average value, which will be derived below from Figure 8.

Figure 5 shows as an example a fit of Equation (1) to the two events of Figures 2 and 3. The data points at 5, 9.4, and 17.4 MeV were taken from the IMP F 6 experiment (Bell Telephone Laboratories), the 94 MeV data points from the IMP F 11 experiment (University of Chicago). The c_1 and c_2 values were calculated from the >10 and >60 MeV t_m values. A similar good fit is obtained for *all* events, the deviations of the individual $v \times t_m$ points from the curves are within the errors of the t_m determination. The character of the majority of the curves is between the two examples shown in Figure 5.

Having determined the c_1 and c_2 values from the 10 and 60 MeV t_m data, it is possible to predict a t_m value for the 30 MeV protons and compare it with the actually observed value. This was done in Figure 6 on two different time scales demonstrating the good correspondence.

If the equation indeed holds for a large number of events it must be concluded that the propagation of solar flare accelerated particles consists of at least two processes, one of which is energy dependent, but independent of flare location, while the other one is energy independent but depends on flare location.

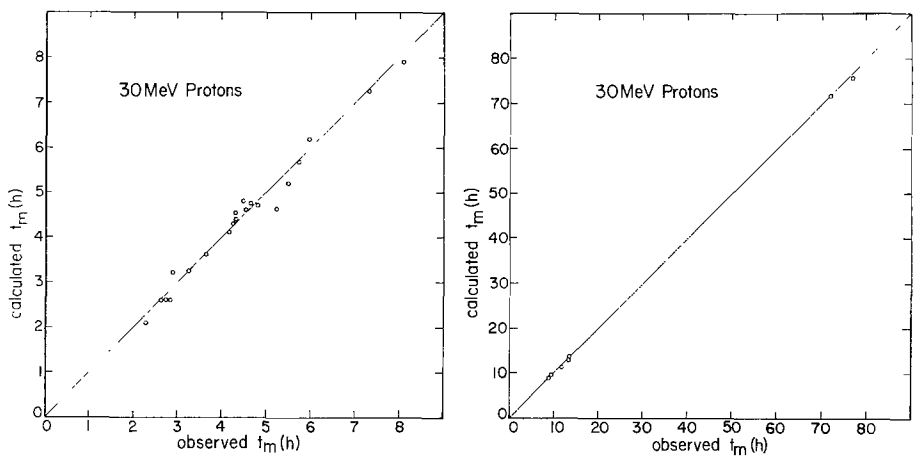

Fig. 6. The c_1 and c_2 values are derived from the t_m data for 10 and 60 MeV protons. Equation (1) is used to calculate the t_m value for the 30 MeV protons from c_1 and c_2; this 'calculated' t_m is plotted vs the actually observed 30 MeV t_m values. The deviations are within the errors of the t_m determination.

A simple comparison of c_1 with the corotation velocity shows that corotation is much too small to account for the observed c_1.

If the observed increase in t_m with $\Delta\phi$ is to be explained by diffusion across the interplanetary magnetic field, one needs large values of the perpendicular diffusion coefficient $K_\perp$. In models by Burlaga (1967) and Lupton and Stone (1973) the fits to the observed azimuthal spread result in $K_\perp \gtrsim K_\parallel$, in contradiction to other experimental results as discussed in the introduction. As such, this is not a general objection against essential interplanetary perpendicular diffusion, because Burlaga and Lupton and Stone have used a particular radial dependence $K_\perp \sim r^2$.

If interplanetary perpendicular diffusion would occur closer to the Sun, e.g. in the solar envelope up to $\approx 30\, R_\odot$ (Lüst and Simpson, 1957; Burlaga, 1969, 1971), one might be able to reconcile the conflicting results on azimuthal effects. This possibility, however, is excluded by the observed *energy independence* of the azimuthal propagation. Theoretical treatments of diffusion across a magnetic field yield $K_\perp \sim v$ (v = particle velocity), where the proportionality constant contains the magnetic field power at zero frequency (Jokipii, 1966, 1967, 1971; Roelof, 1966; Hasselmann and Wibberenz, 1968). This simple result holds in the limit of small gyro-radius, which can be applied here. This means that all models explaining the azimuthal spread of t_m by interplanetary perpendicular diffusion should yield energy-dependent time intensity profiles. This is clearly not observed. The parameter $c_1(\phi)$ which describes the increase of t_m with $\Delta\phi$ is independent of the particle energy as shown above.

In principle we have an interplanetary propagation effect which produces an energy-independent contribution to t_m, namely convection due to the solar wind. If the parallel mean free path is sufficiently small convection and adiabatic deceleration must be taken into account when t_m is determined. For $\lambda_r = 0.01$ AU (independent of energy and of radial distance from the Sun) we find from numerical calculations by Webb *et al.* (1973) that $t_m \sim v^{-0.6}$ for 10–60 MeV protons, which clearly deviates from $t_m \sim v^{-1}$, which we would obtain when convective effects are neglected. Fitting an event to Equation (1) over a limited energy range convection would therefore produce a contribution to the constant c_1. This would result in a systematic correlation between c_1 and c_2, because the importance increases with the time the particles spend in the interplanetary space between the Sun and the Earth. There is no correlation between c_1 and c_2 (Figure 7). We find events with large c_2 and $c_1 \approx 0$ and, on the other hand, events with small c_2 and large c_1. This is found for eastern (full points) as well as for western hemisphere events (open points). To summarize, convection does not contribute significantly to c_1 for western hemisphere events. This is not surprising since convection in principle is not an azimuthal propagation process and can therefore not explain the solar longitudinal dependence of c_1. We are led to the conclusion that azimuthal propagation does not take place in the interplanetary space.

In the following discussion we shall interpret the velocity independent part of the intensity profiles as caused by propagation effects close to the Sun. The velocity dependent component, on the other hand, is interpreted as being mainly due to

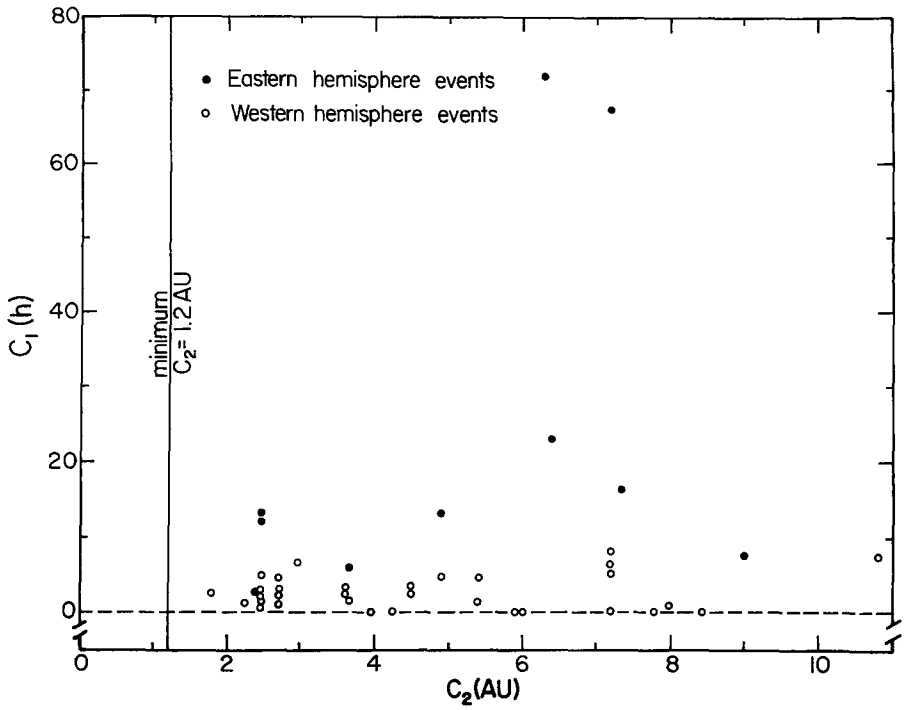

Fig. 7. A plot of c_1 vs c_2 for 43 events. Open points: western, full points: eastern hemisphere. There is obviously no dependence of c_1 on c_2, indicating that the solar and interplanetary processes are separable.

diffusion along the interplanetary magnetic field lines. This separation between the two effects is further supported by the fact that the two components c_1 and c_2, which are obtained from a fit to Equation (1), are independent of each other (see discussion of Figure 7 above). In Section 4 we shall present more evidence to support the idea that c_1 is indeed a solar parameter.

Let us close this section with a discussion of the velocity dependent propagation. In Figure 8 we have plotted c_2 for all events as a function of solar longitude. We see no systematic variation with longitude, the values range from ≈ 2 AU to ≈ 11 AU. We explain this scatter to be produced by variations in the interplanetary magnetic field fluctuations from one event to the other. The c_2 average is 4.6 AU, corresponding to a typical mean free path of $\lambda_r = 0.1$ AU for interplanetary propagation. This value is considerably larger than previously thought of a typical mean free path for interplanetary diffusion, which is consistent with our assumption that in the energy range considered here convective effects are negligible in general, as long as we are only interested in the time profile up to the intensity maximum.

We note that our qualitative arguments are based on a model of interplanetary propagation where the effective radial mean free path λ_r is independent of radial distance from the Sun, at least between the Sun and the Earth. This result is in

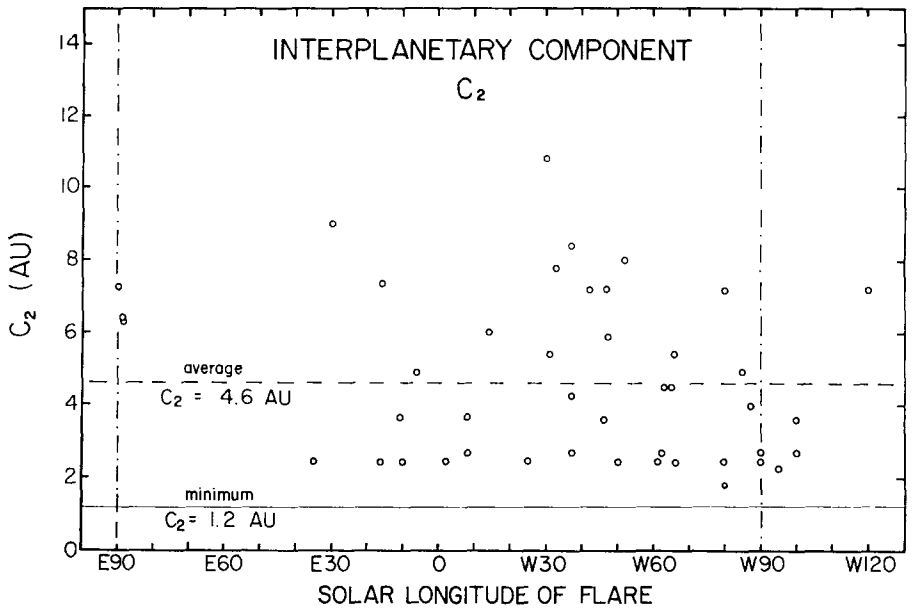

Fig. 8. The interplanetary component c_2 is independent of solar longitude. The minimum value of c_2 corresponds to scatter free particles travelling directly from the Sun to the Earth along the average spiral magnetic field.

agreement with Morfill *et al.* (1972), who have treated the scattering of cosmic ray particles by Alfvén waves propagating out from the Sun. In their model the mean free path is essentially constant within 1 AU.

4. The Solar Component

We now consider the dependence of $c_1(\phi)$ (Figure 9). Although there is significant scatter in the c_1 values for a given solar longitude the increase for eastern hemisphere events is evident. Another characteristic feature is the wide range ($0° \leqslant \phi \leqslant$ W 100°) for events with pure velocity dispersion ($c_1 \approx 0$), the meaning of which will be discussed in Section 5.

The bordering lines drawn in Figure 9 are similar to those drawn in Figure 1. We now have separated the solar propagation and it is possible to obtain a mean coronal transport velocity v_D from the slopes of the bordering lines in the *eastern* hemisphere. After subtracting corotation we find

$$24° \text{ day}^{-1} \leqslant v_D \leqslant 93° \text{ day}^{-1},$$

or

$$3 \text{ km s}^{-1} \leqslant v_D \leqslant 12 \text{ km s}^{-1},$$

if the transport takes place close to the solar surface. The corotation velocity was subtracted from v_D to obtain the bordering lines for events in the invisible hemisphere

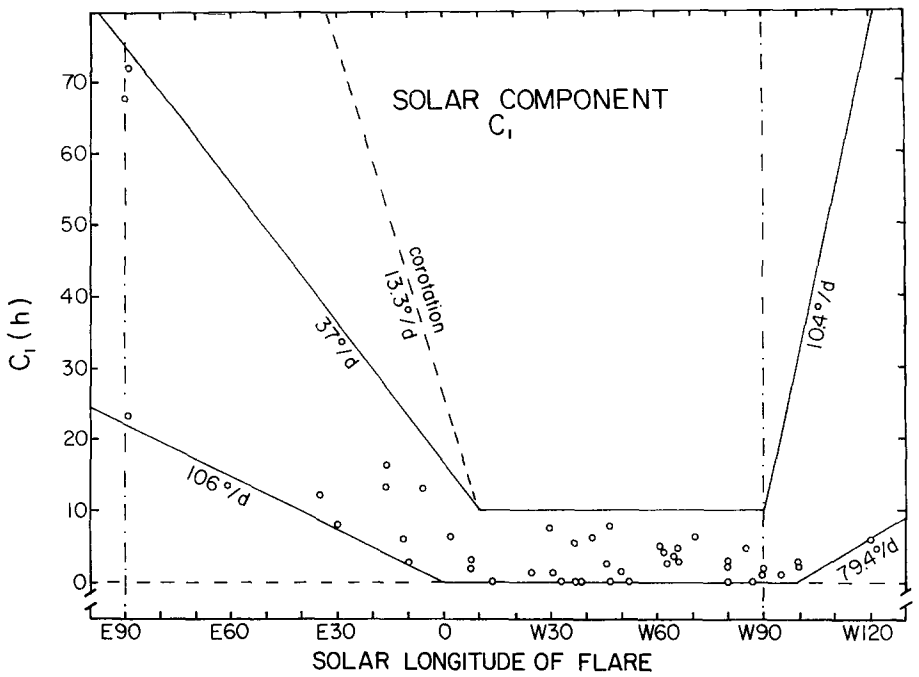

Fig. 9. The solar component. The events in the eastern hemisphere are bordered by lines as in Figure 1. After subtracting the corotation velocity a mean coronal transport velocity of 1–4° h^{-1} is derived from the slopes. The corotation velocity was added to obtain the bordering lines for > W 90°. The events with large c_1 in the western hemisphere are explained by the same coronal transport processes as the eastern hemisphere events. The existence and the extent of the fast propagation region (FPR), where $c_1 \approx 0$, is evident. See also Figure 1.

where flare associations are doubtful (events shown are December 3, 1967, ≈W 100°; November 2, 1969, ≈W 95°; July 7, 1970, ≈W 100°; September 1, 1971, ≈W 120°; the time of particle acceleration was determined from X-ray burst data).

From the analysis of the $c_1(\phi)$ plot alone it is not possible to determine what kind of coronal transport produces the observed dependence. We shall show that diffusive as well as systematic drift processes are effective.

A pure diffusive process will have the following features:

(1) an increase in width of the time intensity profile with increasing $\Delta\phi$ ($\Delta\phi$ is the distance from the flare location to the root of the field line bundle on the Sun, which leads out to an observer in space),

(2) a quadratic dependence of t_m on $(\Delta\phi)^2$,

(3) an intensity maximum at the flare site throughout the event, which is several orders of magnitude higher than at longitudes far away from the flare,

(4) in general the propagation is energy dependent, except if by chance $\lambda \sim 1/v$.

A process of pure convection or drift close to the Sun on the other hand will lead to:

(1) an intensity profile which is independent of the distance from the flare, in particular, the maximum intensity is the same for all longitudes,

(2) a linear dependence of t_m on $\Delta\phi$,

(3) at late times the particle intensity is higher at a longitude away from the flare site than at the flare site,

(4) the propagation is energy independent for convection or an $E \times B$ drift process.

The loss of flare particles into the interplanetary medium has some effect on the time intensity profile as the particles travel through the solar atmosphere. In a model with diffusion and loss (Reid, 1964) there would be a deviation from a $t_m \sim (\Delta\phi)^2$ dependence. If the drift term dominates the diffusion term the t_m dependence on $\Delta\phi$

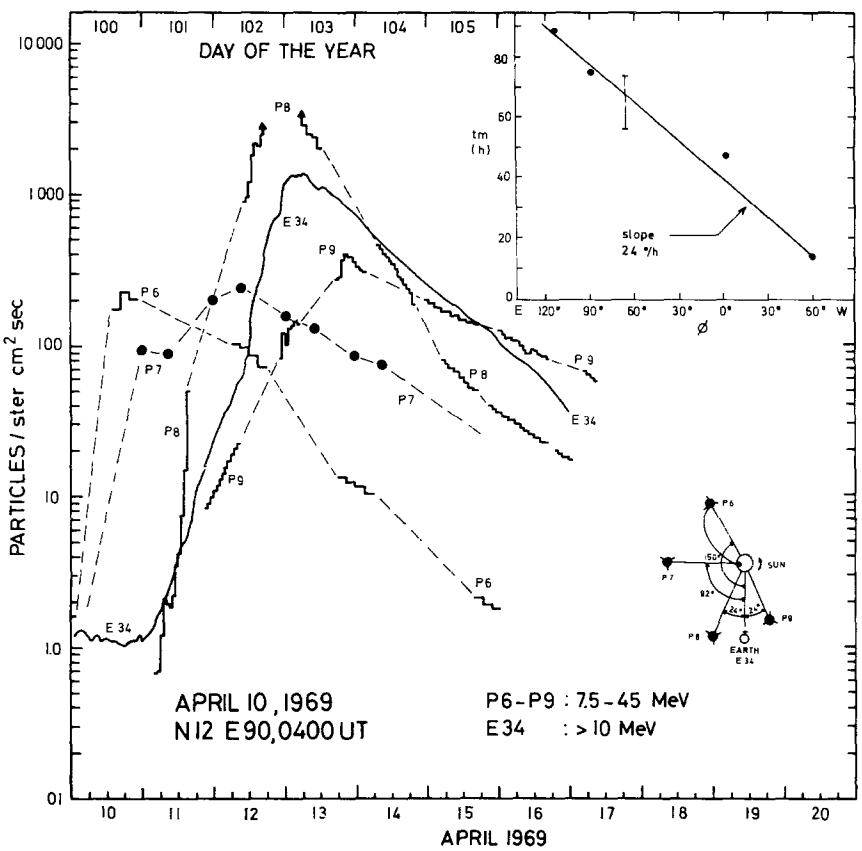

Fig. 10. The consecutive time intensity profiles of the April 10, 1969, E 90° event measured by Pioneers 6–9 and Explorer 34 (IMP F). The positions of the satellites are shown, Pioneer 6 is directly connected with the flare site. The time of maximum particle intensity depends *linearly* on the solar longitude, indicating a dominant large-scale drift process (insert, the longitudes are satellite positions relative to the flare location of E 90°). The slope yields an average coronal transport velocity of $\sim 1.85^{c}\ h^{-1}$. The particle intensities at late times are clearly higher at spacecraft away from the flare site, which gives further evidence for a coronal drift. At the same time diffusion causes the profiles to become wider with increasing time.

would be better represented by a straight line than by a parabola, similar to a drift-diffusion model where the drift term dominates the diffusion term. A straight line dependence does therefore not necessarily support drift. The main difference lies in the decrease of the maximum intensity with distance from the flare, the decrease is several orders of magnitude stronger in the diffusion-loss model than in the diffusion-drift model. When discussing feature (2) it is therefore necessary to analyze the t_m on $\Delta\phi$ dependence together with the decrease of the particle intensity $N_{\max}(\Delta\phi)$ (feature 3). This will be further pursued when Figure 10 will be discussed and also by calculations in Paper II, which show that a straight line dependence indeed would result from drift, since only a small fraction of particles is lost into the interplanetary space.

We now compare the 4 features established above for diffusion and drift with observations. As to feature (1), a simple comparison of typical eastern with western hemisphere profiles gives clear evidence for the existence of diffusive processes in azimuthal propagation: eastern hemisphere events have larger rise and decay times than western hemisphere events, i.e. their profiles cannot be explained by time-shifting of a typical western hemisphere event.

As to feature (2), we note that the bordering lines in Figure 9 can be described by a quadratic as well as by a linear relation between c_1 and ϕ. However, we will discuss now a multi-space probe observation which demonstrates the existence of a drift-type process. Figure 10 shows as an example the April 10, 1969 event observed at E 90°. The particle intensity increases were registered by Pioneers 6–9 and by IMP F over a range in solar longitude of $\approx 175°$. (The Pioneer data were taken from McCracken *et al.* (1971).) The energy thresholds of the Pioneer (7.5–45 MeV) and the IMP F (>10 MeV) channels are not identical, but the differences in the times of maximum intensity due to the different energies are completely negligible. The sub-satellite points, which are the footpoints of the magnetic field lines connecting the satellite with the Sun, are calculated using an average solar wind velocity of 400 km s^{-1}. It is clearly seen that the times of maximum particle intensity increase *linearly* with azimuthal distance of the satellite. The velocity of the convection or drift process is obtained from the slope in the insert of Figure 10, where $t_m(\Delta\phi)$ is plotted. After subtracting the corotation velocity of $0.55° \text{ h}^{-1}$ v_D is found to be $1.85° \text{ h}^{-1}$ which corresponds to 6.27 km s^{-1}, if we locate the position of the process at a height of $1r_s$. This value for v_D lies inbetween the values derived from the $c_1(\phi)$ plot.

We see in Figure 10 that the maximum particle intensity is not observed for the Pioneer 6 spacecraft, which is located close to $\Delta\phi = 0$, but for Pioneer 8 at $\Delta\phi = 125°$. This is an additional argument for the existence of a linear transport process removing particles systematically away from the flare site (feature 3).

This observation is especially interesting, since the peak flux being the highest at $\Delta\phi = 125°$ is neither predicted by pure diffusion nor by pure drift and may be explained by a separate phenomenon, such as the concept of "preferred longitudes of release of particles" (Roelof, 1973).

As to feature (4), the observed energy independence of the azimuthal propagation

also supports a drift type process rather than propagation by diffusion. It is beyond the scope of this paper to analyze the nature of this drift process. Most likely the drift is $E \times B$ drift, which would be consistent with the required energy independence. More multispaceprobe observations will be necessary to decide whether the particles propagate away from the flare site into *all* directions, or it is an *uni*directional transport into a preferred westward or eastward direction. Livingston (1971) has found direct evidence for a westward wind in the solar corona. His observations, however, need further confirmation.

We have derived the existence of a solar drift process from eastern hemisphere events. Let us now discuss some events in the western hemisphere, having unusually large c_1 (Figure 9). In our analysis we have separated the $t_m(v)$ dependence into a velocity dependent and a velocity independent part (c_1). We have interpreted the first part as of interplanetary, the second (c_1) of solar origin. This means that in some events shown in Figure 9 between W 30° and W 70° a large number of particles has spent a time period of 5–7 h close to the Sun.

Let us discuss this problem by introducing another independent observable parameter, the onset time. Onset times of solar events have already been successfully used to describe east–west effects (Simnett, 1971; Lanzerotti, 1973).

Figure 11 shows the relation between c_1 and the onset times t_s of 30 MeV protons for 44 events. The onset of a particle event is most likely connected with particles which have travelled almost scatter free with small pitch angles along the field lines

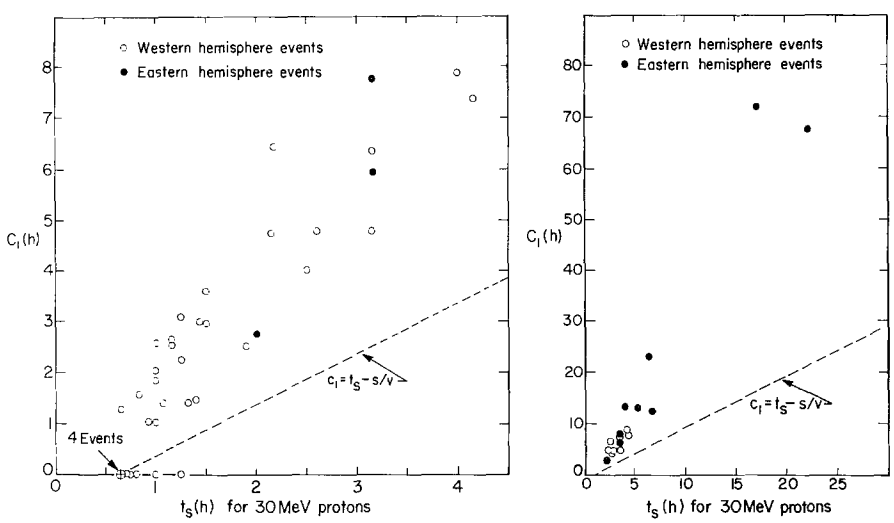

Fig. 11. The two pure *solar* parameters t_s and c_1. t_s is the time difference between the observed particle onset at the spacecraft and the assumed time of acceleration at the flare site. The dashed line is the case of stable storage or pure drift in the solar corona. The c_1/t_s ratios are the same for eastern and western hemisphere events, indicating that the processes giving reason for large c_1 (see Figure 9) are the same for eastern and western hemisphere events, namely coronal transport consisting of drift and diffusion.

between Sun and Earth. Subtracting the direct travel time s/v (s is the path length along the spiral shaped field lines) from the onset time t_s, we have $t_s - s/v$ as the time, where the first particles have left the Sun on the group of field lines leading to the observer. s/v appears as a constant shift of the correlation line in the t_s vs c_1 plot which does not influence the correlation coefficient. Furthermore, s/v is only a small correction (0.67 h for 30 MeV protons) which can be neglected in most cases. t_s is therefore taken as a pure solar propagation parameter.

Now the good correlation between c_1 and t_s in Figure 11 is especially noteworthy. We had previously interpreted c_1 as a measure for the time it takes the bulk of particles to move from the flare site to the foot of an observer's field line. The general increase of t_s with c_1 supports our interpretation of c_1 as a pure solar parameter. On the other hand, we see that in general $t_s - s/v < c_1$. This means that the first particles leave the the Sun *before* the arrival of the bulk of the particles at the same solar longitude. This can be taken as additional evidence that indeed a diffusive process close to the Sun is superimposed on the general drift. This conclusion had so far been based on the broadening of the time profiles with increasing distance from the flare.

In principle, the observed ratio between c_1 and $t_s - s/v$ could be interpreted by a storage process with a gradual leakage of particles out of the storage region. However, the general increase of c_1 with longitude on the eastern hemisphere of the Sun and the discussion of Figure 10 have already led us to the existence of a drift process in the solar atmosphere. Taking the coronal transport velocity of $1.85° \text{ h}^{-1}$ from Figure 10, we see that it takes about 8 h to span a longitudinal distance of 15°. It seems not unreasonable, therefore, to explain the large c_1 values on the western hemisphere by the same drift process derived from eastern hemisphere events.

To summarize this part of the discussion: The solar propagation is a combined drift and diffusion process. This holds for eastern and western hemisphere events.

In the last section we shall discuss a third type of propagation, which leads to equally small t_m values over a wide range of solar longitude.

5. Fast Longitudinal Propagation in the Initial Phase

It was pointed out above (Figure 1, Figure 9, Section 4) that there are 'fast' events with small t_m and $c_1 \approx 0$ over a wide range of solar longitude. The extent of this region is found from Figure 1 to be approximately $0° \leqslant \phi \leqslant \text{W } 100°$. The possibility that the events with small t_m around 0° and W 90° are connected with unusual solar wind speeds leading to large deviations from the nominal Archimedean spiral can be immediately excluded by inspection of the actual solar wind data for these events.

We therefore postulate the existence of a fast azimuthal propagation process on the Sun, which in the initial phase after a flare rapidly transports energetic particles across 40°–50° of solar longitude or fills up a region of that size. The extent of this fast propagation region (FPR) may vary greatly from one event to the other.

Fan *et al.* (1968) arrive at the same conclusion, when they analyzed the propagation of 13–70 MeV protons measured by Pioneer 6 in March 1966. The existence as well as

the same size of the FPR are also found by Krimigis and Verzariu (1971) for low energy protons and by Wang (1972) for 170–1000 keV electrons. The extent of the FPR of $\approx 100°$ is identical with the 'open cone of propagation' found by Anderson and Lin (1966), Lin and Anderson (1967) and Lin (1970) for >40 keV electrons.

If we attempt to understand these observations we must realize that any model has to explain:

(1) the existence of a fast longitudinal propagation,

(2) the finite and variable extent of the FPR.

It is quite possible that two completely different physical processes are involved to explain these two features.

Let us first discuss possible mechanisms for the fast transport. Random walk of field lines as caused by supergranulation of the photosphere (Leighton, 1964; Jokipii and Parker, 1969) yields a mean square displacement of $\langle(\Delta\phi)^2\rangle^{1/2} \approx 6°$ after 12 h. Jokipii and Parker argue that this value is doubled, if ordinary granulation is included, which is still insufficient to explain the wide sector in Figure 1 ($\Delta\phi \approx 50°$ in less than 2 h).

Another possible mechanism for a fast propagation is the transport of particles in thin current sheets (Fisk and Schatten, 1971). According to their estimate, a 10 MeV proton can diffuse across 60° in ≈ 0.5 h, which would be in agreement with the observations. If we assume that the 'open cone of propagation' found for electrons and the FPR found for protons are due to the same mechanism, the application of the current-sheet concept may be questionable, since the gyroradius of a 40 keV electron in a 1 G field in only 6.7 m (the thickness of the current sheet should be smaller than the gyroradius of the particle for the transport to be efficient).

We finally point out the magnetic field configuration diverging from active regions over $\approx 100°$ of solar longitude given as a possible explanation by Fan *et al.* (1968) and Wang (1972). The authors stress that this model should describe only the general direction of the field, but that in addition the magnetic field might be irregular causing significant diffusion. An increase of the FWHM for events inside the FPR is actually observed for events close to the edges of the FPR (Wang, 1972). The diffusion coefficient obtained from the increase of the FWHM for the 170–1000 keV electrons is 3×10^{18} cm^2 s^{-1}, which gives a transit time of 0.1 h for the bulk elctrons for a propagation across 60° in longitude.

At present it is not possible to deduce from the data presented in this paper whether one of the last two processes can explain the FPR. Other mechanisms, such as the transport or release of particles by the shock wave generated in the flare (Athay and Moreton, 1961; Uchida *et al.*, 1973; Palmer and Smerd, 1972) should also be considered.

On the other hand it may not be necessary to introduce a new physical process for the fast propagation. Large magnetic field loops spanning angular distances up to 50° have been frequently observed. Although the energetic particles may be partly trapped during their oscillatory motion along a single loop, gradient and curvature drift could move them to other loop systems, thus providing a rapid and efficient means of transport.

The finite extent of the FPR may be connected with the existence of neutral field lines which can be inferred from Hα maps for the cromosphere (McIntosh, 1972). Roelof and Krimigis (1973) have shown that these neutral field lines serve as boundaries for azimuthal propagation of low energy protons and that, on the average, neutral field lines cross the solar equator every 60°, defining large-scale cells of uniform magnetic polarity. If the fast propagation mode rapidly fills up the cell with particles, the injection regime could extend over as much as 60°. Allowing for variations of the flare location within the cell, an extent of the FPR of $\approx 100°$ is possible. Although we are far from understanding the processes involved, e.g. how high the cromospheric boundaries extend into the corona as compared to the height of the propagation region of the various particle energies we think that the *extent* of the FPR is possibly due to the bordering effect of the neutral field lines.

6. Summary

We have undertaken a systematic analysis of a large number of solar proton events in the energy range of 10–60 MeV from May 1967 through May 1972. Plotting the time of maximum particle intensity t_m vs solar longitude ϕ we find that there is no minimum value for t_m at a particular longitude, instead we find a wide region $0° \leqslant \phi \leqslant$ W 100°, where equally small t_m values are found. This region is interpreted as a fast azimuthal propagation region (FPR), in which the particles can propagate across $\approx 60°$ in solar longitude in less than 1 h in the initial phase after a flare. The finite extent of the FPR may be connected with neutral field lines crossing the solar equator thus defining large scale cells of uniform magnetic polarity. The nature of the rapid transport inside the FPR remains unrevealed. Several possible mechanisms are discussed.

It is found that the variation of t_m is due to both solar and interplanetary propagation processes. These processes are separable, since the variation of t_m for all events can be described by a sum of two components $t_m = c_1 + c_2/v$, which are independent of each other. The first component c_1 is independent of the particle energy but depends on solar longitude, whereas the second component c_2/v depends on the particle energy but is independent of solar longitude.

c_1 describes azimuthal propagation. The observation that c_1 is energy independent disagrees with interplanetary perpendicular diffusion, since $K_\perp \sim v$. The influence of convection in the interplanetary space is considered and found to be negligible in the discussed energy regime. c_1 is therefore interpreted as the coronal transport time for the bulk of the flare particles. This is confirmed by the observation that there is no correlation between c_1 and the interplanetary component c_2 but a good correlation between c_1 and t_s. t_s, the observed particle onset time, is considered to be a pure solar parameter, when the particle travel time in the interplanetary medium is subtracted.

The above interpretation of c_1 implies that the second term c_2/v describes the interplanetary propagation along the field lines. For $c_1 = 0$ (which is only found for events within the FPR) this corresponds to the well-known velocity dispersion $v \times t_m = \text{const}$. We do not claim that the interplanetary propagation is always strictly described by

pure velocity dispersion. Deviations from this over-simplified behaviour may occur for individual events, and this means that the 'bulk coronal transport time' is not always identical with the value c_1 determined from a fit to Equation (1).

The good correlation between c_1 and the particle onset time t_s shows however, that on the average c_1 can be taken as a pure solar parameter. On the other hand this implies that the propagation in the interplanetary medium is well approximated by pure velocity dependence or in a diffusion model by a mean free path length independent of energy.

The character of the coronal transport is revealed when the time intensity profiles of one event as seen by 5 spacecraft are compared. The fluxes at late times are comparable or larger at spacecraft far away from the flare than at spacecraft close to the flare. The times of maximum intensity increase linearly with longitudinal distance with an angular velocity of $1.85° \text{ h}^{-1}$ (the corotation velocity is subtracted), a value which is in agreement with the angular velocities derived from the $c_1(\phi)$ plot. Both observations, the linear increase of t_m with $\Delta\phi$ and the higher maximum intensity away from the flare, cannot be explained by diffusion alone. It is concluded that there are systematic drift processes in the solar corona. These drift processes may not be well ordered, causing the observed general diffusive behaviour. The relative importance of drift and diffusion may vary from one event to the other. Eastern hemisphere events probably are drift dominated events.

Acknowledgements

It is a pleasure to thank Dr E. C. Roelof for many stimulating discussions during the visit of one of us (R.R.) at the University of New Hampshire from December 1972 till March 1973. The flare associations have been carefully checked and compared with the flare associations (mainly due to Drs H. W. Dodson and E. R. Hedeman) of the data catalog prepared by the IUCSTP Working Group 2 (Švestka and Simon, 1974). We are especially indebted to Drs M. A. Shea and D. F. Smart, who made these comparisons possible and were very helpful in giving us some of their data. We would also like to thank Dr J. H. King from the NSSDC, Goddard Space Flight Center, and Dr L. J. Lanzerotti from Bell Telephone Laboratories for making data available. This work is partly supported by the *Deutsche Forschungsgemeinschaft.*

References

Anderson, K. A. and Lin, R. P.: 1966, *Phys. Rev. Letters* **16**, 1121.
Athay, R. G. and Moreton, G. E.: 1961, *Astrophys. J.* **133**, 935.
Axford, W. I.: 1965, *Planetary Space Sci.* **13**, 1301.
Barcus, J. R.: 1969, *Solar Phys.* **8**, 186.
Barouch, E., Engelmann, J., Gros, M., Koch, L., and Masse, P.: 1969, in V. Manno and D. E. Page (eds.), *Proc. of the third ESLAB/ESRIN Symposium*, p. 448.
Barouch, E., Gros, M., and Masse, P.: 1971, *Solar Phys.* **19**, 483.
Bryant, D. A., Cline, T. L., Desai, U. D., and McDonald, F. B.: 1965, *Astrophys. J.* **141**, 478.
Bukata, R. P., Rao, U. R., McCracken, K. G., and Keath, E. P.: 1972, *Solar Phys.* **26**, 229.
Burlaga, L. F.: 1967, *J. Geophys. Res.* **72**, 4449.
Burlaga, L. F.: 1969, *Proc. 11th Int. Conf. on Cosmic Rays*, Mo. 46.
Burlaga, L. F.: 1971, in K. Schindler (ed.), *Proc. of the Conf. on Cosmic Plasma Phys.*, p. 73.

Cline, T. L. and McDonald, F. B.: 1968, *Solar Phys.* **5**, 507.
Datlowe, D.: 1971, *Solar Phys.* **17**, 436.
Dilworth, C., Maccagni, D., Perotti, F., Tanzi, E. G., Mercier, J. P., Raviart, A., Treguer, L., and Gros, M.: 1972, *Solar Phys.* **23**, 487.
Englade, R. C.: 1971, *J. Geophys. Res.* **76**, 768.
Fan, C. Y., Pick, M., Pyle, R., Simpson, J. A., and Smith, D. R.: 1968, *J. Geophys. Res.* **73**, 1555.
Fisk, L. A. and Schatten, K. H.: 1972, *Solar Phys.* **23**, 204.
Hasselmann, K. and Wibberenz, G.: 1968, *Z. Geophys.* **34**, 353.
Jokipii, J. R.: 1966, *Astrophys. J.* **146**, 480.
Jokipii, J. R.: 1967, *Astrophys. J.* **149**, 405.
Jokipii, J. R.: 1971, *Rev. Geophys. Space Phys.* **9**, 27.
Jokipii, J. R. and Parker, E. N.: 1969, *Astrophys. J.* **155**, 777.
Krimigis, S. M. and Verzariu, P.: 1971, *J. Geophys. Res.* **76**, 792.
Krimigis, S. M., Roelof, E. C., Armstrong, T. P., and van Allen, J. A.: 1971, *J. Geophys. Res.* **76**, 5921.
Lanzerotti, L. J.: 1973, 'Coronal Propagation of Low-Energy Solar Protons', preprint.
Leighton, R. B.: 1964, *Astrophys. J.* **140**, 1547.
Lin, R. P.: 1970, *Solar Phys.* **15**, 453.
Lin, R. P. and Anderson, K. A.: 1967, *Solar Phys.* **1**, 446.
Livingston, W.: 1971, *Solar Phys.* **19**, 379.
Lüst, R. and Simpson, J. A.: 1957, *Phys. Rev.* **108**, 1563.
Lupton, J. E. and Stone, E. C.: 1973, *J. Geophys. Res.* **78**, 1007.
McCracken, K. G., Rao, U. R., Bukata, R. P., and Keath, E. P.: 1971, *Solar Phys.* **18**, 100.
McIntosh, P. S.: 1972, *Rev. Geophys. Space Phys.* **10**, 837.
McKibben, R. B.: 1972, *J. Geophys. Res.* **77**, 3957.
Morfill, G., Alpers, W., and Völk, H. J.: 1972, *AGU Fall Annual Meeting*, SC 16.
Obayashi, T.: 1964, *Space Sci. Rev.* **3**, 79.
Palmer, I. D. and Smerd, S. F.: 1972, *Solar Phys.* **26**, 460.
Rao, U. R., McCracken, K. G., Allum, F. R., Palmeira, R. A. R., Bartley, W. C., and Palmer, I.: 1971, *Solar Phys.* **19**, 209.
Reid, G. C.: 1964, *J. Geophys. Res.* **69**, 2659.
Roelof, E. C.: 1966, Thesis, Physics Department, University of California, Berkeley.
Roelof, E. C. and Krimigis, S. M.: 1973, *J. Geophys. Res.* **78**, 5375.
Sakurai, K.: 1971, 'Energetic Electrons from the Active Region McMath No. 8905 during 20 July and 5 August, 1967', preprint GSFC X-693-71-268.
Simnett, G. M.: 1971, *Solar Phys.* **20**, 448.
Solar Geophysical Data, U.S. Department of Commerce, Boulder, Colo. 80302.
Švestka, Z. and Simon, P. (eds.): 'Catalog of Solar Particle Events, 1955–1969', D. Reidel Publ. Comp., Dordrecht, in press.
Uchida, Y., Altschuler, M. D., and Newkirk, G.: 1973, *Solar Phys.* **28**, 495.
Wang, J. R.: 1972, 'The Coronal Transport of the Flare-Associated Scatter-Free Electrons', preprint GSFC X-661-72-76.
Webb, S., Balogh, A., Quenby, J. J., and Sear, J. F.: 1973, *Solar Phys.* **29**, 477.